A NEW ANALYSIS FOR MEMBRANE NOISE

THE INTEGRAL SPECTRUM

LOUIS J. DEFELICE *and* BARRY A. SOKOL

From the Department of Anatomy, Emory University, and School of Electrical Engineering, Georgia Institute of Technology, Atlanta, Georgia 30322

ABSTRACT A new method of random data analysis has been developed with special implications for membrane noise. The integral spectrometer uses overlapping broadband filters of simple design, whose bandwidth increases linearly with center frequency. A random two-state process, which has a Lorentzian-shaped spectral density, results in an integral spectrum whose maximum value occurs at the mean frequency of the events, and which is symmetric about that frequency on a semilog plot. $1/f$ noise is flat and does not distort the symmetry on the frequency axis. The integral spectrum exchanges resolution on the frequency axis for accuracy in the amplitude. The expected statistical error in amplitude has been calculated for three types of membrane noise assuming finite data. The integral spectrum compares favorably with conventional spectral densities and may be a reasonable alternative for random data analysis.

INTRODUCTION

The study of membrane noise, as a reflection of the molecular events associated with excitability, has enjoyed a period of growth since the pioneering work of Verveen and Derksen (1968, for an early review). We have yet to see the elementary conductance change directly, as one apparently can do in synthetic membranes. The statistical sum of many events, in the form of membrane noise, is the closest we have come to this goal (Verveen and DeFelice, 1974).

Theoretical models have been developed which relate the elementary membrane events to the power spectral density of the noise, or to its integral over frequency, the variance. However, power spectral density measurements are limited in accuracy by the duration of the data, which experimental conditions usually restrict to a few minutes or less. It is now evident that power spectral density estimates are not sufficiently accurate to distinguish between available models.

The present paper describes a new method of noise analysis, called an integral spectrum, which may have advantages over conventional methods for membrane noise. This method may be favorably applied to any noise signal whose spectral density does not contain much structure. For example, reaction noise from a chemical process (Feher and Weissman, 1973) could be analyzed by the integral spectrum method.

It may not always be advantageous to use the integral spectrum instead of the spectral density. For signals which have discrete frequency components, the frequencies at which peaks occur in the integral spectrum may be shifted from their original values. In addition, the integral spectrum may not resolve frequency components which are close to each other. Curve-fitting could be used to regain the original information, but a normal spectral analysis would have been easier.

THEORY

Estimates of the conventional spectral density are derived from finite data by filtering. By definition, the filters are required to be narrow. The amplitude of the spectral density is the square of the filter output averaged over time. Analysis shows that the narrower the filter, the greater the expected error in amplitude. Long averaging times may reduce this error, but often the length of data is fixed by other requirements, especially in a biological preparation. Another error, usually ignored, derives from the nonideal filter shape, albeit sharply peaked at some frequency.

It therefore may be reasonable to consider a simple broadband filter whose form and effect on noise data are easily calculated. Such a filter, peaked at some frequency, may be highly nonideal from the point of view of spectral density analysis, and yet may result in useful and even superior noise data reduction. We describe such a filter and its use below.

Definition of the Integral Spectrum

Consider the simplest of realizable band-pass filters, composed of an R_2C_2 low-pass network ideally buffered to a C_1R_1 high-pass network. The voltage transfer function is:

$$Y(if) = (if/f_1)/(1 + if/f_1)(1 + if/f_2), \tag{1}$$

where $f_1 = 1/2\pi R_1C_1$ and $f_2 = 1/2\pi R_2C_2$. Let $f_1 = f_2 = l$. The resulting network, represented by L, has a square modulus given by:

$$|L(f,l)|^2 = (f^2/l^2)/(1 + f^2/l^2)^2. \tag{2}$$

The filter described by Eq. 2 is peaked at the frequency $f = l$ and is symmetric about its peak value on a log f plot.

The integral spectrum is defined by the relation:

$$I(l) = \int_0^\infty S(f)|L(f,l)|^2\,\mathrm{d}f, \tag{3}$$

where $S(f)$ is the true spectral density of a random process.

By analogy with the spectral density, we may also define the integral spectral density by:

$$\int_0^\infty S(f)|L(f,l)|^2\,\mathrm{d}f \Big/ \int_0^\infty |L(f,l)|^2\,\mathrm{d}f = I(l)/(\pi/4)l. \tag{4}$$

Notice that the bandwidth of the L-filter increases linearly with its peak frequency l.

Error Analysis

It is required to find the normalized statistical error ϵ associated with the integral spectrum measured for finite observation time T. We follow Bendat and Piersol (1971).

Let $x(t)$ represent the noise after passing through a particular filter L. The correlation function of the filtered noise is given by:

$$C(\tau) = \int_0^\infty S(f)|L|^2 \cos(2\pi f \tau)\,\mathrm{d}f, \tag{5}$$

where C depends on l and where $C(0)$ is identical to Eq. 3. By definition:

$$C(\tau) = \lim_{T\to\infty} (1/T) \int_0^T x(t)x(t+\tau)\,\mathrm{d}t. \tag{6}$$

We define the integral spectrum for a sample time T as:

$$\hat{I} = (1/T) \int_0^T x^2(t)\,\mathrm{d}t, \tag{7}$$

and the true integral spectrum as:

$$I = \lim_{T\to\infty} \hat{I}. \tag{8}$$

The normalized mean square error is defined by the relation:

$$\epsilon^2 = \langle(\hat{I} - I)^2\rangle/I^2, \tag{9}$$

where $\langle\ \rangle$ indicate an expectation value and may be considered as an average over time. Since $\langle(\hat{I} - I)^2\rangle = \langle(\hat{I})^2\rangle - I^2$, it is only required to evaluate $\langle(\hat{I})^2\rangle$ to find an exsion for ϵ, once I^2 is known.

Now:

$$\begin{aligned}\langle(\hat{I})^2\rangle &= \left\langle(1/T) \int_0^T x^2(t)\,\mathrm{d}t(1/T) \int_0^T x^2(t)\,\mathrm{d}t\right\rangle \\ &= (1/T^2)\left\langle\int_0^T \int_0^T x^2(t)x^2(t')\,\mathrm{d}t\mathrm{d}t'\right\rangle \\ &= (1/T^2) \int_0^T \int_0^T \langle x^2(t)x^2(t')\rangle\mathrm{d}t\mathrm{d}t'.\end{aligned} \tag{10}$$

Notice that the integrand of Eq. 10 is the correlation function of $x^2(t)$. Rice (1945), Eq. 3.9-7, has shown that:

$$\langle x^2(t)x^2(t')\rangle = C^2(0) + 2C^2(\tau), \tag{11}$$

where $\tau = t - t'$.

Therefore:

$$\langle(\hat{I})^2\rangle = C^2(0) + (2/T^2)\int_0^T\int_0^T C^2(\tau)\,dt\,dt'. \quad (12)$$

It may be shown, where $z = x - y$, that:

$$\int_0^T\int_0^T f(x-y)\,dx\,dy = \int_{-T}^0 (T+z)f(z)\,dz + \int_0^T (T-z)f(z)\,dz$$

$$= \int_{-T}^T (T - |\tau|)f(z)\,dz. \quad (13)$$

Since $C^2(0) = I^2$, Eq. 12 becomes:

$$\langle(\hat{I})^2\rangle = I^2 + (2/T)\int_{-T}^T [1 - (|\tau|/T)]C^2(\tau)d\tau, \quad (14)$$

which, for T much larger than $|\tau|$, may be approximated by:

$$\langle(\hat{I})^2\rangle - I^2 \simeq (2/T)\int_{-\infty}^{\infty} C^2(\tau)\,d\tau. \quad (15)$$

Therefore, Eq. 9 becomes:

$$\epsilon^2 = (2/T)\int_{-\infty}^{\infty} C^2(\tau)\,d\tau/I^2(l), \quad (16)$$

which is an estimate of the normalized mean square error associated with the output of a particular filter in an integral spectrometer.

We now apply formulas 5 and 16 to three cases of interest in membrane noise.

White Noise

Let the true spectral density of a process be given by:

$$S(f) = a. \quad (17)$$

The correlation function of white noise band-limited by a particular L-filter is:

$$C(\tau) = \int_0^\infty a[(f^2/l^2)/(1 + f^2/l^2)^2]\cos(2\pi\tau f)\,df$$

$$= al\int_0^\infty [r^2/(1 + r^2)^2]\cos(2\pi\tau lr)dr$$

$$= (al\pi/4)(1 - 2\pi\tau l)e^{-2\pi\tau l}. \quad (18)$$

The integral spectrum is Eq. 18 evaluated at $\tau = 0$; therefore:

$$I(l) = (a\pi/4)l, \quad (19)$$

which is a result already used in Eq. 4. The mean square error is given by Eqs. 18 and 19, squared and substituted into Eq. 16. This results in:

$$\begin{aligned}\epsilon^2 &= (2/T) \int_{-\infty}^{\infty} (1 - 2\pi\tau l)^2 e^{-4\pi\tau l}\, \mathrm{d}\tau \\ &= (4/2\pi l T) \int_0^{\infty} (1 - u)^2 e^{-2u}\, \mathrm{d}u \\ &= 1/2\pi l T. \end{aligned} \tag{20}$$

The integral spectrum for white noise of spectral density a, measured from sample data which exists for time T, is therefore given by:

$$\hat{I}(l) = (a\pi/4)l \pm [1/(2\pi l T)^{1/2}]. \tag{21}$$

1/f Noise

Proceeding as above, let:

$$S(f) = b/f. \tag{22}$$

It can be shown that the correlation function of b/f noise band-limited by a particular L-filter is given by:

$$C(\tau) = (b/2)[1 - \pi\tau l \bar{E}(2\pi\tau l)], \tag{23}$$

where:

$$\bar{E}(u) = e^{-u} Ei(u) - e^{u} Ei(-u), \tag{24}$$

and:

$$Ei(u) = \int_{-\infty}^{u} (e^t/t)\, \mathrm{d}t. \tag{25}$$

Eq. 25 represents the exponential integrals Ei for $u > 0$ and $\bar{Ei}$ for $u < 0$, tabulated in Jahnke and Emde (1945). Note that $1/2\ \bar{E}(u)$ is the asymmetrical part of the function $e^{-u} Ei(u)$. Fig. 1 is a plot of $\bar{E}(u)$ vs. u from which the behavior of Eq. 23 is easily deduced.

The integral spectrum is Eq. 23 evaluated at $\tau = 0$. Since $\bar{E}(0) = 0$,

$$I(l) = b/2. \tag{26}$$

The mean square error is given by:

$$\begin{aligned}\epsilon^2 &= (2/T) \int_{-\infty}^{\infty} (1 - \pi\tau l \bar{E})^2\, \mathrm{d}\tau \\ &= (4/2\pi l T) \int_0^{\infty} [1 - (u/2)\bar{E}]^2\, \mathrm{d}u. \end{aligned} \tag{27}$$

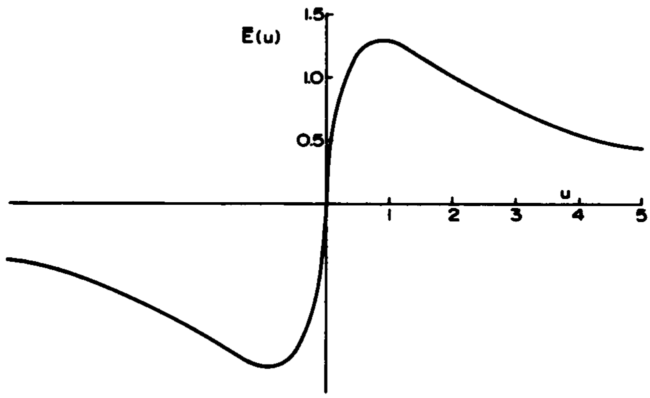

FIGURE 1 A plot of $\bar{E}(u)$, defined by Eqs. 24 and 25, vs. u. $\bar{E}(\infty) = 0$ and $d\bar{E}/du \rightarrow \infty$ at $u = 0$.

It is readily demonstrated that:

$$\int_0^{\infty} [1 - (u/2)\bar{E}]^2 \, du < 2 \int_0^{u_0} [1 - (u/2)\bar{E}] \, du, \tag{28}$$

where u_0 is the first root of Eq. 23, satisfying $u_0 \bar{E}(u_0) = 2$. The only other root is at infinity. A numerical evaluation of the integral in Eq. 27 gives the value 0.6163 ..., and therefore:

$$\epsilon^2 \simeq 2.4652/2\pi l T. \tag{29}$$

The integral spectrum for noise of spectral density b/f, measured from sample data which exists for time T, is given by:

$$\hat{I}(l) = (b/2) \pm [1.57/(2\pi l T)^{1/2}]. \tag{30}$$

Lorentzian (Relaxation) Noise

Let:

$$S(f) = c/[1 + (f/f_0)^2], \tag{31}$$

where $1/2\pi f_0$ is the relaxation time constant. The correlation function corresponding to Eq. 31, band-limited by a particular L-filter, is calculated to be:

$$C(\tau) = \frac{c\pi l^2 f_0^2}{2(l^2 - f_0^2)} \left\{ \frac{l e^{-2\pi\tau l} - f_0 e^{-2\pi\tau f_0}}{l^2 - f_0^2} - \frac{1}{2l}(1 - 2\pi\tau l) e^{-2\pi\tau l} \right\}. \tag{32}$$

The integral spectrum is Eq. 32 evaluated at $\tau = 0$; therefore:

$$I(l) = (c\pi/4)[l/(1 + l/f_0)^2]. \tag{33}$$

The mean square error is given by a rather lengthy but straightforward calculation; the result is:

$$\epsilon^2 = (1/2\pi T l)\{(5p^3 + 1 + 3p - 9p^2)/(p + 1)(p - 1)^2\}, \tag{34}$$

where $p = l/f_0$. The following conditions are useful:

$$
\begin{aligned}
&l \ll f_0 && \epsilon^2 \to 1/2\pi T l \\
&l = f_0 && \epsilon^2 = 3/2\pi T f_0 \\
&l \gg f_0 && \epsilon^2 \to 5/2\pi T l.
\end{aligned} \tag{35}
$$

The error decreases uniformly with l.

The integral spectrum for noise of spectral density $c/[1 + (f/f_0)^2]$, measured from sample data which exists for time T, is given by:

$$\hat{I}(l) = (c\pi/4)[l/(1 + l/f_0)^2] \pm [\sqrt{\{\ \}}/(2\pi T l)^{1/2}], \tag{36}$$

where { } is as written in Eq. 34.

DISCUSSION

To summarize the results, the integral spectrum corresponding to:

$$S(f) = a + (b/f) + (c/[1 + (f/f_0)^2]) \tag{37}$$

is given by:

$$I(l) = (a\pi/4)l + (b/2) + (c\pi/4)[l/(1 + l/f_0)^2]. \tag{38}$$

Operationally, exactly the same thing is implied in measuring both the conventional spectral density $S(f)$ and the new integral spectrum $I(l)$. For each, the noise is passed through a set of filters whose output is squared and averaged over time. For $S(f)$, the filters are narrow, with as little overlap as possible, and the average squared output is divided by the filter bandwidth and plotted vs. the filter center frequency (f). For $I(l)$, the filters are broad and overlap extensively; the average squared output is plotted vs. the filter center frequency (l), without division by the filter bandwidth.

Notice that $fS(f)$ has a frequency dependence similar to $I(l)$:

$$fS(f) = af + b + (cf/[1 + (f/f_0)^2]). \tag{37 A}$$

The advantage of spectral *shape* of $I(l)$ is therefore not a sufficient reason to use it. For example, Lorentzian noise analyzed as an integral spectrum is peaked at $l = f_0$ and is symmetric about f_0 on a log l plot. Also, $1/f$ noise is flat and does not shift the Lorentzian on the frequency axis. But these properties are also shared by replotting $S(f)$ along the lines indicated by Eq. 37 A. Similarly, the frequency dependence of $4I(l)/\pi l$ is close to that of $S(f)$; for:

$$4I(l)/\pi l = a + (2b/\pi l) + [c/(1 + l/f_0)^2]. \tag{38 A}$$

Eq. 38 A has graphical properties very similar to Eq. 37. White and $1/f$ noise have identical behavior to the conventional spectral density. On a log l plot, the Lorentzian in Eq. 38 A has limiting slopes of 0 and -2 at low and high frequencies, respectively, but f_0 defines the 1/4 power point (6 dB down) rather than the 1/2 power point (3 dB down) as in the conventional spectral density. The significant difference between Eqs. 37 and 38 A or between Eqs. 38 and 37 A lies in their respective errors.

The errors for each term in Eq. 38 are given in Eqs. 21, 30, and 36. Spectral density errors also depend on the specific form of $S(f)$; see, e.g., Bendat and Piersol (1971), Eq. 6.98. However, the dominant term for the normalized mean square error for $S(f)$ at every f is simply:

$$\epsilon^2 = 1/BT, \tag{39}$$

where B is the bandwidth of the *narrow filter* centered at f. Analyzers are often manufactured with B constant.

To compare the expected error in $S(f)$ with that in $I(l)$ for a Lorentzian spectrum, consider the ratios of their normalized mean square errors; from Eqs. 35 and 39:

$$\begin{aligned} l \ll f_0 \qquad & (1/BT)/(1/2\pi Tl) = 2\pi l/B \\ l = f_0 \qquad & (1/BT)/(3/2\pi Tf_0) = 2\pi f_0/3B \\ l \gg f_0 \qquad & (1/BT)/(5/2\pi Tl) = 2\pi l/5B. \end{aligned} \tag{40}$$

As an example, take $B = 2.5$ Hz and $f_0 = 31.6$ Hz as shown in Fig. 2; then $2\pi f_0/3B \simeq 26$, which implies that, at the cut-off frequency, the expected error in $S(f)$ is at least five times that of $I(l)$ for the same length of data. It is reasonable to expect conventional analysis always to imply $B < f_0$. Similar relationships exist for white and $1/f$ noise, and are readily calculated from the formulas given.

To test this analysis, a spectrometer was made from 5% decade resistor and capacitor boxes properly buffered, and an rms meter which can respond to low frequencies. The correlation functions derived above, namely Eq. 18, 23, and 32, were all checked against measurements with an HP 3721A correlator, whose $\tau = 0$ values were then used for the integral spectrum plots. A simple experimental noise model was con-

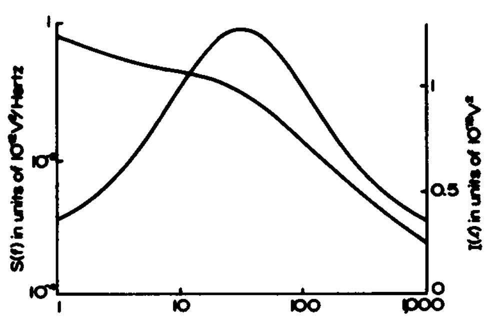

FIGURE 2 The theoretical functions log $S(f)$ and $I(l)$ vs. the logarithm of frequency, for $S(f) = b/f + c/[1 + (f/f_0)^2]$ and $I(l) = b/2 + (c\pi l/4)/(1 + l/f_0)^2$. The values $b = 5 \times 10^{-13}$ V^2, $c = 1.64 \times 10^{-13}$ V^2/Hz, and $f_0 = 31.6$ Hz were used. These correspond to the experimental model of Figs. 3 and 4.

structed and the resulting integral spectra were compared with a conventional analysis using a Honeywell SAI 52C spectrum analyzer.

White plus $1/f$ noise was generated by a 200 kΩ carbon composition resistor in parallel with a two-volt source with 200 kΩ internal resistance. The white noise source was therefore Johnson noise from 100 kΩ; the $1/f$ noise source was due to energy dissipation in the resistor (DeFelice, 1976). Lorentzian noise was generated by a 10 MΩ resistor in parallel with a 500 pF capacitor. These two sources, white plus $1/f$ noise and Lorentzian noise, were detected by low-noise voltage preamplifiers and were summed and amplified in subsequent stages. The expected values are: $a = 4kT$ (100 kΩ) = 1.64×10^{-15} V²/Hz; $c = 4kT$ (10 MΩ) = 1.64×10^{-13} V²/Hz; and $f_0 = 31.6$ Hz. b is controlled by the current through the 200 kΩ resistors and was selected at $b = 5 \times 10^{-13}$ V² to compete with the Lorentzian. These values of b and c were used to construct Fig. 2.

Fig. 3 *a* shows the voltage spectral densities from the white plus $1/f$ source and from the Lorentzian source, measured conventionally. Fig. 3 *b* shows the composite spectral density. Each spectrum represents approximately 2 min of data and each is the average of 64 spectra. The data in Fig. 3 are plotted on a linear frequency axis to give an equal density of points across the spectrum. These points are connected by a solid line. The more usual representation for power spectral densities is a log-log plot (see Fig. 2). A replot cannot change the fundamental error in a spectrum. To extract the param-

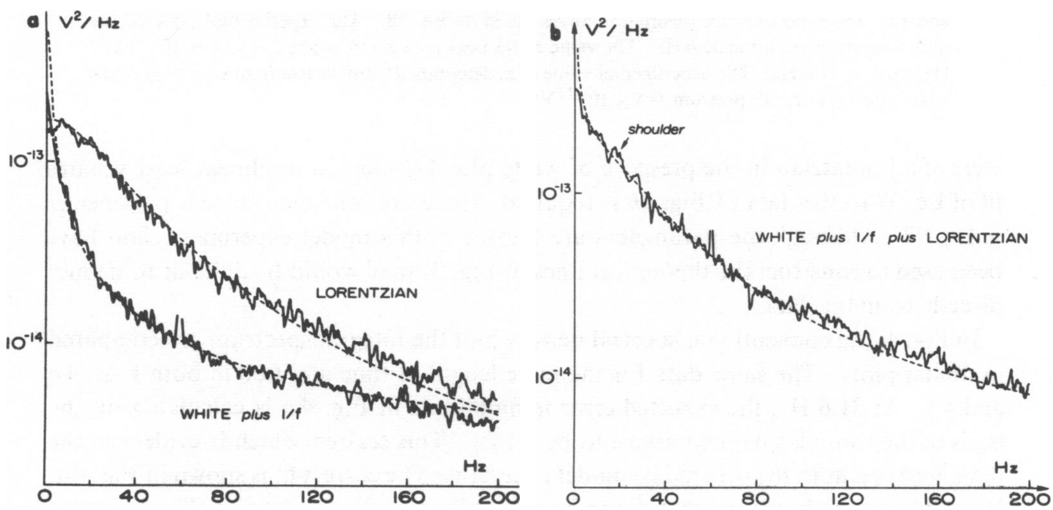

FIGURE 3*a* FIGURE 3*b*

FIGURE 3 *a* Measured voltage spectral densities from two model noise circuits. For each spectrum, 128 s of analog data are represented; Hamming windows were used (cosine² on an 8% pedestal) and the average of 64 spectra was taken. The dashed lines are theoretical Lorentzian and white plus $1/f$ spectra constructed from the known parameters of the model.

FIGURE 3 *b* A measured voltage spectral density from the same noise data represented in Fig. 3 *a*, added together before analysis. The same parameters apply. The dashed line is theoretical.

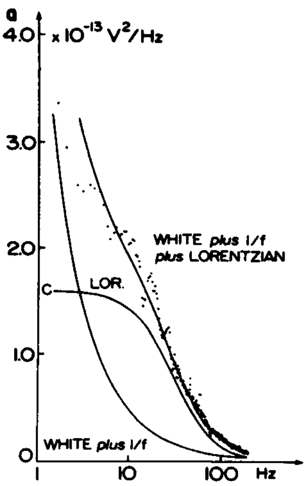

FIGURE 4*a*

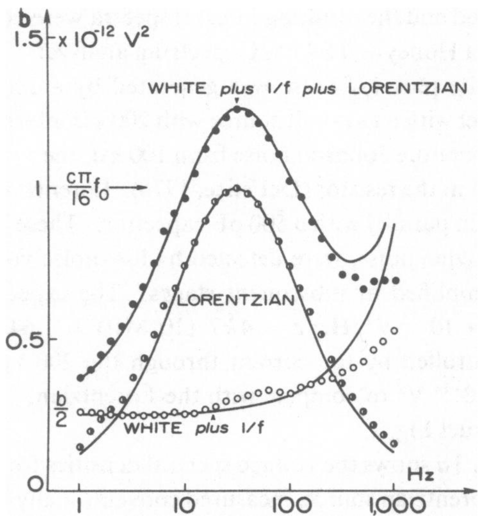

FIGURE 4*b*

FIGURE 4 *a* A measured voltage spectral density from the same data represented in Fig. 3 *b*. A semilog plot is used to facilitate comparison with Fig. 4 *b*. The 400 data points are shown explicitly. The correct composite theoretical curve and the two underlying components are also shown.

FIGURE 4 *b* A measured voltage integral spectra from the same noise data represented in Figs. 3 and 4 *a*. The two lower curves correspond to Fig. 3 *a*, and the upper curve corresponds to Figs. 3 *b* and 4 *a*. The solid lines are theoretical curves based on Eq. 38. The experimental peak of the pure Lorentzian occurs at 31.6 Hz. The value at the peak is $c\pi f_0/16$, where $c = 1.64 \times 10^{-13}$ V²/Hz and $f_0 = 31.6$ Hz. The experimental value of *b*, determined from the low frequency limit of the white plus $1/f$ integral spectrum, is 5×10^{-13} V².

eters of a Lorentzian in the presence of white plus $1/f$ noise, a nonlinear least squares fit of Eq. 37 to the data of Fig. 3*b* is required. There are four independent parameters in Eq. 37. Although the parameters are known in this model experiment, and have been used to construct the theoretical lines in Fig. 3, they would be difficult to deduce directly from the data.

In Fig. 4, the conventional spectral density and the integral spectrum are compared in similar plots. The same data for the same length of time are used in both Figs. 4 *a* and 4 *b*. At 31.6 Hz, the expected error in amplitude in Fig. 4 *a* is calculated on the basis of the formulas derived above to be ±14%. This scatter, which is evident in the data, makes a fit to the theoretical model uncertain. The correct fit is shown in Fig. 4 *a*. It can be shown, however, that f_0 can be determined from the data in Fig. 4 *a* to no better than ±50%. By comparison, the expected error in the integral spectrum amplitude at the peak frequency is ±1.2%. It can be shown that f_0 can be determined from the data in Fig. 4 *b* to within ±8% of the known correct value.

To test the new method further, membrane current noise preserved on magnetic tape and already published has been reanalyzed. Fig. 5 in the present paper represents the same data as the spectral density in Fig. 4 of DeFelice et al. (1975). The data was taken

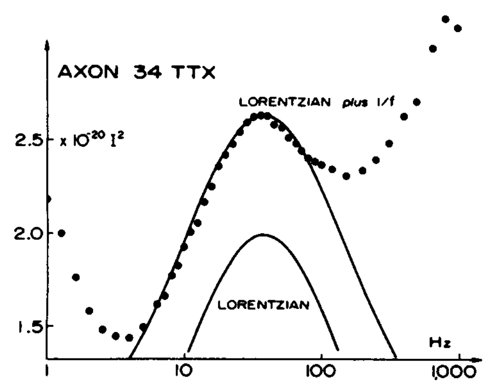

FIGURE 5 A measured current integral spectrum. The experimental points are a reanalysis of current noise from squid giant axon under voltage clamp and in the presence of TTX, which has already been published as a spectral density. Membrane area = 0.28 cm^2, temperature = 8.6°C, voltage = −53 mV. The resting potential for this membrane was −61 mV. The solid lines are theoretical integral spectra whose absolute values for b, c, and f_0 match those in Fig. 4 of DeFelice et al., 1975.

under voltage clamp in the presence of TTX from the squid giant axon. The integral spectrum easily detects an underlying Lorentzian which appears as an obvious peak in Fig. 5. The tailing-up at higher frequencies is due primarily to amplifier voltage noise and membrane capacitance. The similar effect below the peak is due to the low frequency instabilities in the data. One main advantage of the new method is the accuracy of the experimental curve for the same length of data. This accuracy should allow the necessary corrections of Fig. 5 to be made with much greater precision. However, we confine ourselves to comparison with the $1/f$ and Lorentzian components already published, using the same ratio of c/b (equal to 0.207 at 1 Hz) and value of f_0 (38 Hz) to calculate theoretical integral spectra.

SUMMARY

The new mathematical transformation, defined by Eqs. 2 and 3, has been shown to be of practical significance in the analysis of membrane noise. Theoretical results now available suggest that noise measurements may be used to distinguish between different molecular models of ionic conduction in excitable membranes (Hill and Chen, 1972; Stevens, 1972; Chen and Hill, 1973; Chen, 1975, in preparation). Recent experiments which attempt to do this with conventional spectra density analysis are not sufficiently accurate to make the required distinctions (Wanke et al., 1974; DeFelice et al., 1975; Conti et al., 1975; Siebenga et al., 1973; van den Berg et al., 1976). Since $I(l)$ is uniquely related to $S(f)$ through Eq. 3 and since the statistical error in I is greatly improved over that of S for the same length of data, the methods suggested in this paper may be helpful. New attempts to compare theory with experiment will undoubtedly require nonlinear curve-fitting procedures unlike the rather crude graphical tech-

niques previously used. It would seem evident that the better determined the experimental curve, the greater the significance of such procedures.

This work was supported in part by National Institutes of Health grants LM 02505 and NS 05669.

Received for publication 25 July 1975 and in revised form 12 February 1976.

REFERENCES

BENDAT, J. S., and A. G. PIERSOL. 1971. *Random Data: Analysis and Measurement Procedures.* Wiley-Interscience, New York.

CHEN, Y-D., and T. L. HILL. 1973. Fluctuations and noise in kinetic systems. *Biophys. J.* **13**:1276.

CONTI, F., L. J. DEFELICE, and E. WANKE. 1975. Potassium and sodium ion current noise in the membrane of the squid giant axon. *J. Physiol. (Lond.).* **248**:45.

DEFELICE, L. J. 1976. 1/f-resistor noise. *J. Appl. Phys.* **47**:350.

DEFELICE, L. J., E. WANKE, and F. CONTI. 1975. Potassium and sodium current noise from squid axon membranes. *Fed. Proc.* **34**:1338.

FEHER, G., and M. WEISSMAN. 1973. Fluctuation spectroscopy: determination of chemical reaction kinetics from the frequency spectrum of fluctuations. *Proc. Natl. Acad. Sci. U.S.A.* **70**:870.

HILL, T., and Y-D. CHEN. 1972. On the theory of ion transport across the nerve membrane. IV. Noise from the open-close kinetics of K channels. *Biophys. J.* **12**:948.

JAHNKE, E., and F. EMDE. 1945. *Tables of Functions.* Dover Publications, New York.

RICE, S. O. 1945. Mathematical analysis of random noise. *Bell Syst. Tech. J.* **24**:46.

SIEBENGA, E., A. MEYER, and A. A. VERVEEN. 1973. Membrane shot-noise in electrically depolarized nodes of Ranvier. *Pfluegers Arch. Gesamte Physiol.* **341**:87.

STEVENS, C. F. 1972. Inferences about membrane properties from electrical noise measurements. *Biophys. J.* **12**:1028.

VAN DEN BERG, R. J., J. DE GOEDE, and A. A. VERVEEN. 1975. Conductance fluctuations in Ranvier nodes. *Pfluegers Arch. Gesamte Physiol.* **360**:17.

VERVEEN, A. A., and L. J. DEFELICE. 1974. Membrane Noise. *In* Progress in Biophysics and Molecular Biology. J. A. V. Butler and D. Noble, editors. Pergamon Press, Oxford. **28**:189.

VERVEEN, A. A., and H. E. DERKSEN. 1968. Flucutation phenomena in nerve membrane. *Proc. IEEE.* **56**:906.

WANKE, E., L. J. DEFELICE, and F. CONTI. 1974. Voltage noise, current noise and impedance in space clamped squid axon. *Pfluegers Arch. Gesamte Physiol.* **347**:63.